

Core/Shell SiO_x@PAM Nanospheres from UV-Assisted Surface-Initiated Free Radical Polymerization

Peng Liu, Liuxue Zhang, Zhixing Su

Institute of Polymer Science and Engineering, College of Chemistry and Chemical Engineering, Lanzhou University, Lanzhou, Gansu 730000, People's Republic of China

Received 17 February 2005; accepted 20 April 2005

DOI 10.1002/app.22078

Published online in Wiley InterScience (www.interscience.wiley.com).

ABSTRACT: The core/shell SiO_x@polyacrylamide (SiO_x@PAM) nanospheres were successfully prepared by the in situ surface-initiated free radical polymerization of acrylamide (AM) from the silica nanoparticles with self-assembled monolayers (SAMs) of *N*-methyl aniline (NMA) in presence of benzophenone via a precipitation polymerization method under the ultraviolet (UV) irradiation. The conversion of monomer (C%) and the percentage of encapsulating (PE%), calculated from the elemental analyses (EA) results, reached 20.9 and 51.0% after 150 min of UV-irradiation, respectively. It is consistent with the analyses of TGA. Fourier transform infrared

(FTIR) analyses also confirmed the formation of the core/shell SiO_x@PAM nanospheres. And it was investigated that the silica nanoparticles had been encapsulated with PAM from the X-ray photoelectron spectrometer (XPS) analyses. The analysis results of transmission electron microscope (TEM) showed that the diameters of the SiO_x@PAM nanospheres were in the range of 50–200 nm. © 2006 Wiley Periodicals, Inc. *J Appl Polym Sci* 100: 3433–3438, 2006

Key words: core/shell; SiO_x@PAM nanospheres; surface-initiated radical polymerization; ultraviolet irradiation

INTRODUCTION

Polymer-modified inorganic nanoparticles have received some interests in a wide range of industrial field, such as diagnosis, electronics, toner, and paint application because of their functionality and dispersion stability properties.^{1–4} Moreover, they have better electrical, magnetic, thermal, and optical properties and extend their range of industrial applications.^{5–8} Grafting polymers on to inorganic nanoparticles provides better mechanical properties such as strength, shape, and chemical resistance.⁹

With the “grafting from” methods, polymer-grafted inorganic nanoparticles had been successfully prepared by the “one-pot” method,¹⁰ macro-monomer method¹¹ and macro-chain transfer agent method.¹² Much attention is being focused on densely grafted polymer brushes through surface-initiated polymerization (SIP), such as macro-initiator method,^{13–15} in which chain growth is promoted from initiating groups already attached to the surfaces. This is mainly because in the former ap-

proach, initially grafted chains (at the beginning of adsorption) sterically shield remaining active sites on surfaces, resulting in limited graft density and thickness of polymer brushes.¹⁶ The advantage of SIP is that high-density polymer brushes are accessible where the average distance between grafting points is much smaller than the radius of gyration (R_g).

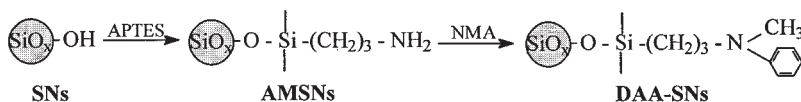
UV-initiated surface photografting polymerization is a facile and efficient method in solid surface modification. With the distinct advantages, forming fast covalent bonds between the new graft layers and the substrate surface, but doing little damage to the material's bulk properties, this method has attracted much attention since the pioneering work of Oster in 1957.¹⁷ By the graft method, the surfaces of solid substrates can be planted with a layer of new polymer chains with various functional groups in very short time according to the requirements for modification applications.

The UV-assisted surface-initiated free radical polymerization^{18–20} and controlled/“living” radical polymerization techniques^{21–23} had been successfully used for the graft polymerizations of vinyl monomers from the surfaces of films and particles. Here, we reported the preparation of core/shell SiO_x@polyacrylamide (SiO_x@PAM) nanospheres by the surface photo-induced radical polymerization of acrylamide (AM) from the *N,N*-dialkyl aniline-modified silica nanoparticles (DAA-SNs) under the ul-

Correspondence to: P. Liu (pliu@lzu.edu.cn).

Contract grant sponsor: Natural Science Foundation, Gansu Province; contract grant number: 3ZS041-A25-002.

Contract grant sponsor: Interdisciplinary Innovation Research Fund for Young Scholars, Lanzhou University; contract grant number: LZU200302.



Scheme 1 The self assembly procedure to DAA-SNs.

traviolet (UV) irradiation in the presence of benzophenone as coinitiator.

EXPERIMENTAL

Materials and reagents

The silica nanoparticles (SN) used was MN1P, obtained from Zhoushan Mingri Nano-materials, Zhejiang, China. The surface area, particle size, and silanol group content were $640 \text{ m}^2 \text{ g}^{-1}$, 10 nm, and 48%, respectively. It was dried in vacuum at 110°C for 48 h before use.

γ -Aminopropyltriethoxysilane (APTES) (Gaizhou Chemical Industrial, Liaoning, China) was used without further purification. The monomer AM and the coinitiator benzophenone were all recrystallized from ethanol. *N*-methyl aniline (NMA), toluene, and ethanol used were all analytical grade from Tianjin Chemical Reagent, China.

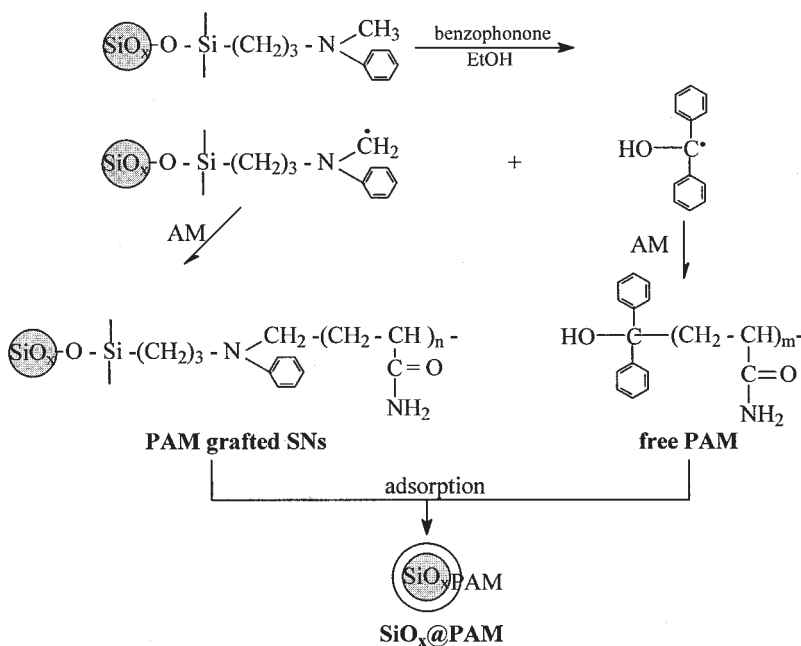
Preparation of the macro-initiator

γ -Aminopropyl silica nanoparticles (APSNs) was prepared by the self-assembly of APTES onto the surfaces of silica nanoparticles.²⁴

The macro-initiators, DAA-SNs, were prepared by the self assembly of *N*-methyl aniline (NMA) onto aminopropyl silica nanoparticles (AMSNs) by refluxing with NMA in toluene, according to the method reported previously.²⁵ The products were separated by being centrifuged at 1.0×10^4 rpm for 1 h and dispersed in ethanol with ultrasonic vibration and recentrifuged. The preparation procedure to the macro-initiators could be summarized as shown in Scheme 1.

Surface-initiated free radical polymerizations

The mixture of 1.50 g DAA-SNs, 1.00 g benzophenone, 5.00 g AM, and 100 mL ethanol was dispersed with ultrasonic vibration for 10 min. Then, the mixture was stirred with an electromagnetic stirrer at ambient temperature (about 20°C) under a 300 W high-pressure mercury lamp (qe6 , $\lambda = 365 \text{ nm}$, Osram Corp., Germany) with a distance of 15 cm. The mixture N_2 was bubbled throughout the polymerizing period. After a given polymerizing time, the product was removed, washed with large masses of ethanol, and dried in vacuum at 40°C . The encapsulation of the silica nanoparticles with both the grafted and the adsorbed PAM could be summarized as shown in Scheme 2.



Scheme 2 The encapsulation procedure.

In the comparing experiments, only the same amounts of AM and benzophenone or AM, AMSNs, and benzophenone were dispersed into ethanol with ultrasonic vibration, and then the mixture were irradiated under UV lamp with the same distance.

Analyses and characterizations

Elemental analysis (EA) of C, N, and H was performed on Elementar vario EL instrument. Bruker IFS 66 v/s infrared spectrometer was used for the Fourier transform infrared (FTIR) spectroscopy analysis. The surface characterization of the *c*-PS-SNs was accomplished using a PHI-5702 multi-functional X-ray photoelectron spectrometer (XPS) with pass energy of 29.35 eV and an Mg K α line excitation source. The binding energy of C 1s (284.6 eV) was used as a reference. The surface elemental compositions were determined from the peak area ratios and were accurate to within 1%. The morphology of the bare silica nanoparticles and the SiO_x@PAM nanospheres were characterized with a JEM-1200 EX/S transmission electron microscope (TEM). The powders were dispersed in toluene in an ultrasonic bath for 5 min, and then deposited on a copper grid covered with a perforated carbon film. Thermogravimetric analysis (TGA) were used for the thermal stability of the PAM-grafted silica nanoparticles, the SiO_x@PAM nanospheres, and the pure PAM performed with a Perkin-Elmer TGA-7 system at a scan rate of 10°C min⁻¹–800°C in N₂.

Polymerization parameters

The PAM-grafted silica nanoparticles were separated by the extraction of the SiO_x@PAM nanospheres with distilled water, similar as reported previously.¹⁰

The conversion of monomer (C%), the percentage of encapsulating (PE%), and the efficiency of grafting (EG%) were calculated from the results of elemental analyses (EA) according to the following relationships:

$$C (\%) = \text{Total PAM (g)}/\text{monomer used (g)} \times 100\%$$

$$PE (\%) = \text{PAM shell (g)}/\text{inorganic core (g)} \times 100\%$$

$$EG (\%) = \text{Grafted PAM (g)}/\text{total PAM (g)} \times 100\%$$

RESULTS AND DISCUSSION

The core/shell SiO_x@polyacrylamide (SiO_x@PAM) nanospheres were successfully prepared using a two-step method. In the first step, the macro-initiators, DAA-SNs, were prepared by the self assembly of *N*-methyl aniline (NMA) onto aminopropyl silica nanoparticles (AMSNs), with a content of 3.20 mmol g⁻¹,

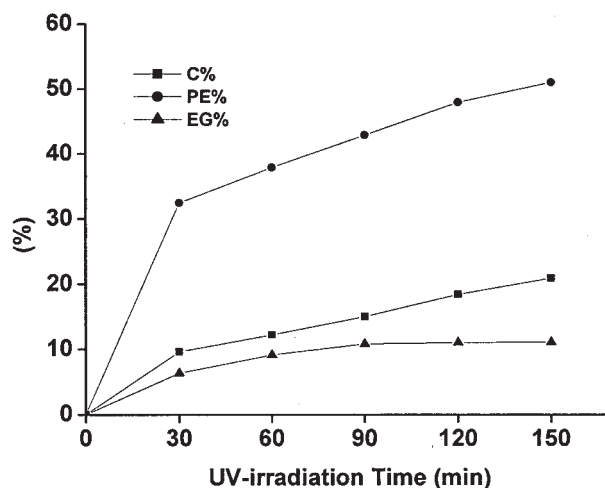


Figure 1 The effects of the UV-irradiation time on the C%, PE%, and EG%.

according to the EA results. And then in the second step, the UV-assisted surface-initiated free radical polymerization of AM was conducted in the presence of benzophenone as coinitiator.

By controlling UV irradiation time, the polymerization evolutions of this system were investigated in detail, and the effect of the UV irradiation time on the C%, PE%, and EG% was shown in Figure 1. The C%, PE%, and EG% increased with the increase of the UV-irradiation time and reached 20.9, 51.0, and 11.0% after 150 min UV-irradiation, respectively. Comparing and analyzing the curves shown in the Figure, the following features were to be noted. High reaction rate at the early stage of polymerization were observed, and no induction period can be observed. The reaction rate was high in the first few minutes and then levels off. With the UV irradiation, a great deal of free radicals were yielded in a short time and used to initiate the polymerization of AM. Therefore, the induction period appearing in normal free radical polymerization was replaced by a high-speed conversion period in this system. After this stage, the polymerization rate decreases gradually, and a final conversion was reached. It may be resulted from the following reasons. The coinitiator, benzophenone, had been used up or the *N,N*-dialkyl aniline groups on the surfaces of DAA-SNs had been enwrapped by the PAN-shell formed.

However, about 80% of the encapsulating PAM could be washed out from the SiO_x@PAM nanospheres, after being washed with water. It indicated that the 80% encapsulating PAM was adsorbed onto the surfaces of the silica nanoparticles without chemical bond. The possible mechanism was followed. Those free polymers, which had been adsorbed but not grafted onto the surface of the inorganic core, were formed by the polymerization of AM, the monomer

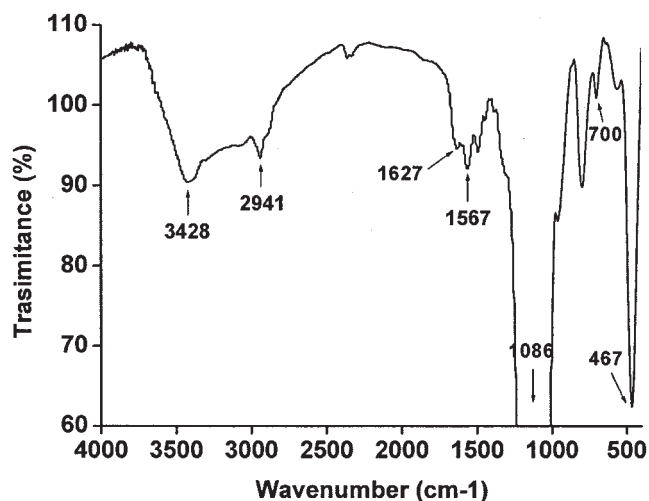


Figure 2 FTIR spectrum of the $\text{SiO}_x\text{@PAM}$ nanospheres.

with high active for photopolymerization under UV irradiation, with the initiation of the benzophenone ketyl radical, a product in the photoreduction of benzophenone although it was less active than the *N,N*-dialkyl aniline radical. The latter was immobilized onto the surface of the silica nanoparticles, and there was bigger space-hindrance for the addition polymerization of the monomer. So, a mass of the free PAM were formed and adsorbed onto the PAM-grafted silica nanoparticles (PAM-grafted SNs) cores in the polymerizing period.

In the comparing experiments, there was found no polymerization of AM without DAA-SNs added (only AM and benzophenone or AM, AMSNs, and benzophenone in ethanol). It was concluded that the photopolymerization of AM had been initiated by the system containing both benzophenone and the *N,N*-dialkyl aniline groups on the surfaces of DAA-SNs. And, the formation mechanism of the core/shell $\text{SiO}_x\text{@PAM}$ nanospheres could be summarized as shown in Scheme 2.

The band at 700 cm^{-1} of phenyl groups and the band at 1320 cm^{-1} of tertiary amine groups were found in the FTIR spectrum of the micro-initiators, after the self-assembly of NMA onto the surfaces of AMSNs. The FTIR spectrum of the $\text{SiO}_x\text{@PAM}$ nanospheres was shown in Figure 2. The peaks for the carbonyl stretch at 1627 cm^{-1} , the N—H stretch at 3428 cm^{-1} and bend at 1567 cm^{-1} , the aliphatic C—H stretch at 2941 cm^{-1} of PAM and also the phenyl groups at 700 cm^{-1} were found in the FTIR spectrum of the $\text{SiO}_x\text{@PAM}$ nanospheres. The vibration bands corresponding to silica (1086 and 467 cm^{-1}) were found in both the FTIR spectra. It indicated that the nanospheres were composed of PAM and SiO_x .

The X-ray photoelectron spectroscopy (XPS) analysis was consistent with the results from the FTIR

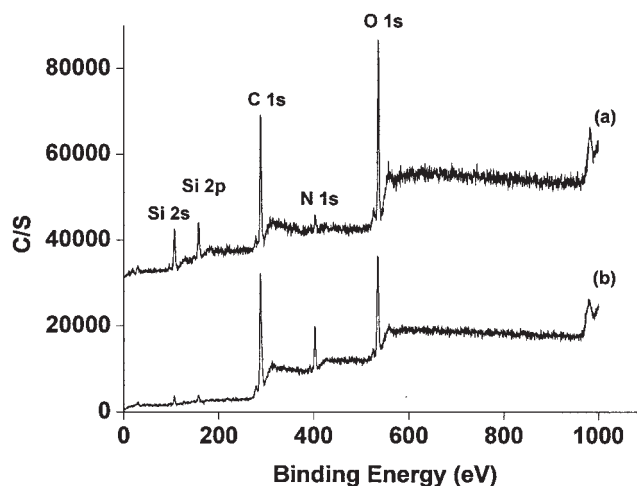


Figure 3 XPS survey of (a) the DAA-SNs and (b) the $\text{SiO}_x\text{@PAM}$ nanospheres.

analyses. The surface compositional data of the DAA-SNs and the $\text{SiO}_x\text{@PAM}$ nanospheres, determined by XPS, were shown in Figure 3 and summarized in Table I. The surface element contents of C and N increased to 63.45 and 11.41% and those of Si and O decreased to 2.98 and 22.16% from the C, N, Si, and O content of 50.15, 3.63, 14.00, and 32.23% of the DAA-SNs and 28.69, 0, 19.94, and 51.09% of the bare silica nanoparticles (SNs), respectively, after the UV-assisted surface-initiated free radical polymerization of AM from the surfaces of the DAA-SNs and the self assembly of NMA onto the surface of the bare silica nanoparticles. It indicated that the silica nanoparticles had been encapsulated by the PAM formed.

The transmission electron microscope (TEM) images of the bare SNs and the $\text{SiO}_x\text{@PAM}$ nanospheres were shown in Figure 4. The diameters of the $\text{SiO}_x\text{@PAM}$ nanospheres were in the range of 50–200 nm. It was much bigger than the 10 nm of the bare SiO_x nanoparticles. It may be due to the aggregations of the PAM-grafted SNs and the insoluble free PAM. It was expected to achieve unique $\text{SiO}_x\text{@PAM}$ nanospheres with ultrasonic vibration in the period of UV-irradiation by the proposed method.

TABLE I
The Surface Compositional Data from XPS

Samples	XPS analysis (at %)			
	Si	O	C	N
Bare SNs	19.94	51.09	28.69	-
DAA-SNs	14.00	32.23	50.15	3.63
$\text{SiO}_x\text{@PAM}$	2.98	22.16	63.45	11.41

The thermal stabilities of the PAM-grafted silica nanoparticles, the $\text{SiO}_x\text{@PAM}$ nanospheres, and the pure PAM were investigated by the TGA analyses (Fig. 5). The weight loss of them at the temperature $<100^\circ\text{C}$ showed the desorption of moist adsorbed from air. The C%, PE%, and EG% values, calculated from the TGA results, were consistent with those from the EA results. It could also be found that the thermal stability of PAM had been improved after the encapsulation on the silica nanoparticle cores.

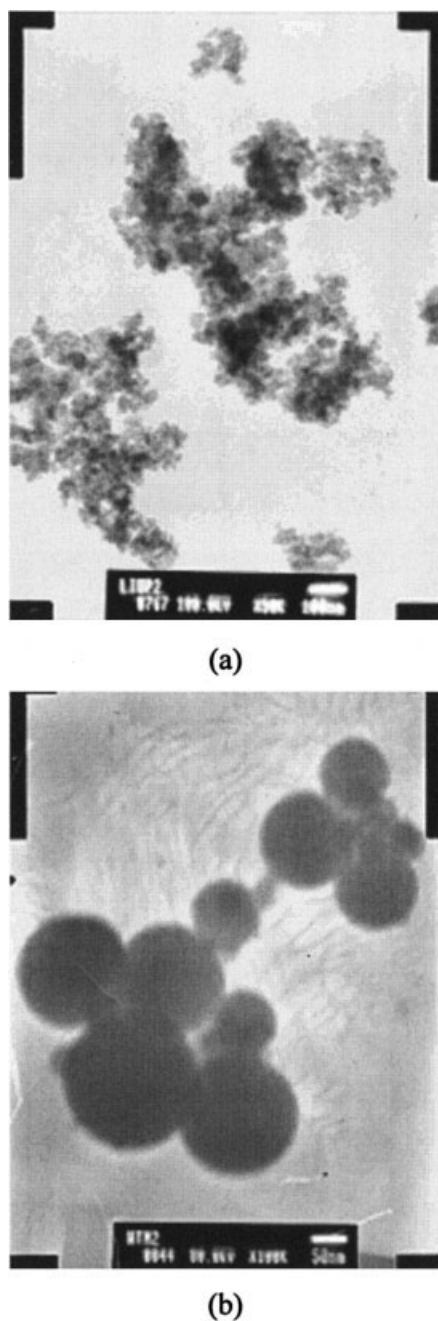


Figure 4 TEM images of (a) the bare SNs and (b) the $\text{SiO}_x\text{@PAM}$ nanospheres.

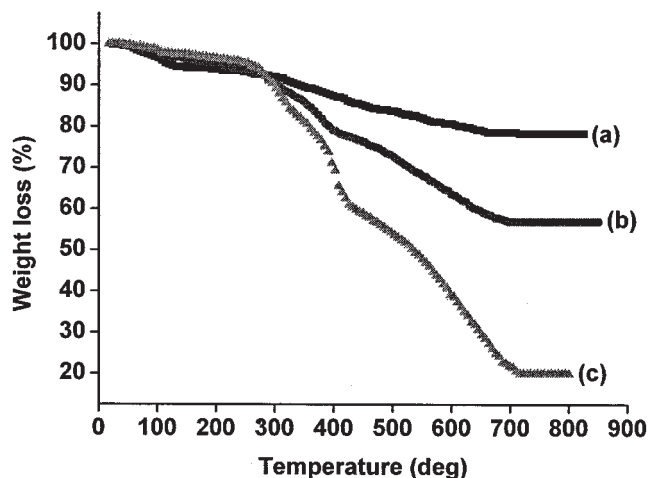


Figure 5 The thermal stabilities of (a) the grafted silica nanoparticles, (b) the $\text{SiO}_x\text{@PAM}$ nanospheres, and (c) the pure PAM.

CONCLUSIONS

The in situ UV-assisted surface-initiated free radical polymerization of AM was conducted from the surfaces of the macroinitiators, DAA-SNs, under the UV irradiation in the presence of benzophenone as coinitiator. The $\text{SiO}_x\text{@PAM}$ nanospheres were obtained via the proposed precipitation polymerization method. All the analysis results from EA, FTIR, XPS, TEM, and TGA indicated the formation of the core/shell $\text{SiO}_x\text{@PAM}$ nanospheres. It was expected to achieve unique $\text{SiO}_x\text{@PAM}$ nanospheres with ultrasonic vibration in the period of UV-irradiation by the proposed method.

References

- Xu, H.; Yan, F.; Monson, E. E.; Kopelman, R. J. *Biomed Mater Res A* 2003, 66, 870.
- Kin, K. M.; Park, N. G.; Kwang, S. R.; Soon, H. C. *Polymer* 2002, 43, 3951.
- Horn, D.; Rieger, J. *Angew Chem Int Ed* 2001, 40, 4330.
- Allen, N. S.; Edge, M.; Sandoval, G.; Ortega, A.; Liauw, C. M.; Stratton, J.; McIntyre, R. B. *Polym Degrad Stab* 2002, 76, 305.
- Cho, M. S.; Park, S. Y.; Hwang, J. Y.; Choi, H. J. *Mater Sci Eng C* 2004, 24, 15.
- Kato, Y.; Sugimoto, S.; Shinohara, K. I.; Tezuka, N.; Kagotani, T.; Inomata, K. *Mater Trans* 2002, 43, 406.
- Zheng, L.; Kasi, R. M.; Farris, R. J.; Coughlin, E. B. *J Polym Sci: Polym Chem* 2002, 40, 885.
- Lu, C. L.; Cui, Z. C.; Wang, Y.; Li, Z.; Guan, C.; Yang, B.; Shen, J. C. *J Mater Chem* 2003, 13, 2189.
- Rong, M. Z.; Zhang, M. Q.; Wang, H. B.; Zeng, H. M. *J Polym Sci: Polym Phys* 2003, 41, 1070.
- Liu, P.; Tian, J.; Liu, W. M.; Xue, Q. J. *Polym J* 2003, 35, 379.
- Liu, P.; Tian, J.; Liu, W. M.; Xue, Q. J. *Mater Res Innov* 2003, 7, 105.

12. Liu, P.; Liu, W. M.; Xue, Q. J. *Eur Polym Mater* 2004, 40, 267.
13. Tsubokawa, N.; Ishida, H. *J Polym Sci: Polym Chem* 1992, 30, 2241.
14. von Werne, T.; Patten, T. E. *J Am Chem Soc* 2001, 123, 7497.
15. Liu, P.; Liu, W. M.; Xue, Q. J. *J Macromol Sci Pure Appl Chem*, 2004, A41, 1001.
16. Balazs, A.; Lyatskaya, Y. *Macromolecules* 1998, 31, 6676.
17. Oster, G.; Shibata, O. *J Polym Sci* 1957, 26, 233.
18. Liang, L.; Rieke, P. C.; Fryxell, G. E.; Liu, J.; Engehard, M. H.; Alford, K. L. *J Phys Chem B* 2000, 104, 11667.
19. Rohr, T.; Hilder, E. F.; Donovan, J. J.; Svec, F.; Frechet, J. M. J. *Macromolecules* 2003, 36, 1677.
20. Peng, Y.; Deng, J. Y.; Yang, W. T. *Macromol Chem Phys* 2004, 205, 1096.
21. de Boer, B.; Simon, H. K.; Werts, M. P. L.; van der Vegte, E. W.; Hadziioanou, G. *Macromolecules* 2000, 33, 349.
22. Liu, P.; Tian, J.; Liu, W. M.; Xue, Q. J. *Polym Int* 2004, 53, 127.
23. Liu, P.; Su, Z. X. *J Photochem Photobiol A Photochem* 2004, 167, 237.
24. Liu, P.; Xur, Q. J.; Tian, J.; Liu, W. M. *Chin J Chem Phys* 2003, 16, 481.
25. Liu, P.; Pu, Q. S.; Sun, Q. Y.; Su, Z. X. *Anal Sci* 2003, 19, 409.